Published in final edited form as:

Nat Immunol. 2016 November ; 17(11): 1322–1333. doi:10.1038/ni.3540.

An essential role for IL-2 receptor in regulatory T cell function

Takatoshi Chinen[#1], **Arun K. Kannan**[#2], **Andrew G Levine**[1], **Xiying Fan**[1], **Ulf Klein**[3], **Ye Zheng**[4], **Georg Gasteiger**[1,5], **Yongqiang Feng**[1], **Jason D. Fontenot**[6,8], and **Alexander Y. Rudensky**[1,8]

[1]Howard Hughes Medical Institute and Immunology Program, Memorial Sloan Kettering Cancer Center, New York, NY, USA

[2]Immunology Discovery, Biogen, Cambridge, MA, USA

[3]Herbert Irving Comprehensive Cancer Center, Department of Pathology and Cell Biology, and Department of Microbiology and Immunology, Columbia University, New York, NY, USA

[4]Nomis Foundation Laboratories for Immunobiology and Microbial Pathogenesis, The Salk Institute for Biological Studies, La Jolla, CA, USA

[5]Institute for Medical Microbiology and Hygiene, University of Mainz Medical Centre, Mainz, Germany

[6]Exploratory Biology, Juno Therapeutics, Seattle, WA, USA

[#] These authors contributed equally to this work.

Abstract

Regulatory T (T_{reg}) cells, expressing abundant amounts of the IL-2 receptor (IL-2R), are reliant on IL-2 produced by activated T cells. This feature implied a key role for a simple network based on IL-2 consumption by T_{reg} cells in their suppressor function. However, congenital deficiency in IL-2R results in reduced expression of the T_{reg} cell lineage specification factor Foxp3, confounding experimental efforts to understand the role of IL-2R expression and signaling in T_{reg} suppressor function. Using genetic gain and loss of function approaches, we demonstrate that IL-2 capture is dispensable for control of $CD4^+$ T cells, but is important for limiting $CD8^+$ T cell activation, and that IL-2R dependent STAT5 transcription factor activation plays an essential role in T_{reg} cell suppressor function separable from T cell receptor signaling.

[8]Corresponding authors. Alexander Y. Rudensky, HHMI and Immunology Program, Memorial Sloan Kettering Cancer Center, 417 East 68th Street, New York, NY 10065, USA., rudenska@mskcc.org, Phone: 646-888-3109 FAX: 646-422-0453, Jason D. Fontenot, Juno Therapeutics, 307 Westlake Avenue North, Seattle, WA 98109, USA, jason.fontenot@junotherapeutics.com, Phone: 206-566-5670.

Author contributions

T.C., J.D.F. and A.Y.R. conceived the project and designed the experiments; T.C., A.K.K., A.G.L., X.F., Y.Z., G.G., and Y.F. conducted experiments; U.K. generated *Il2rb*^{fl} allele; J.D.F. generated *Il2ra*^{fl} allele; T.C., J.D.F. and A.Y.R. wrote and edited the manuscript.

Competing financial interests

The authors declare no competing financial interests.

Accession codes

GSE84553

Regulatory T (T_{reg}) cells expressing the transcription factor Foxp3 restrain immune responses to self and foreign antigens[1-3]. T_{reg} cells express abundant amounts of the interleukin 2 receptor α-chain (IL-2Rα; CD25), but are unable to produce IL-2. IL-2 binds with low affinity to IL-2Rα or the common γ -chain (γ_c)-IL-2Rβ heterodimers, but receptor affinity increases ~1,000 fold when these three subunits together interact with IL-2[4]. IL-2 and STAT5, a key IL-2R downstream target, are indispensable for Foxp3 induction and differentiation of T_{reg} cells in the thymus[5-11]. IL-2Rβ and γ_c are shared with the IL-15 receptor, whose signaling can also contribute to the induction of Foxp3[12]. IL-2, in cooperation with the cytokine TGF-β, is also required for extrathymic T_{reg} cell differentiation[13].

While the role for IL-2R signaling in the induction of Foxp3 expression and T_{reg} cell differentiation in the thymus has been well established by previous studies, the significance of IL-2R expression in mature T_{reg} cells is not well understood. Although the deficiency in STAT5 abolishes Foxp3 expression, it can be rescued by increased amounts of the anti-apoptotic molecule Bcl2. This finding raised a possibility that a primary role for IL-2 is in the survival of differentiating T_{reg} cells or their precursors[14]. It was also reported that ablation of the proapoptotic protein Bim can rescue T_{reg} cells or their precursors from apoptosis associated with IL-2 or IL-2R deficiency and restore T_{reg} cell numbers, but it did not prevent fatal autoimmunity[15]. However, a profound effect of a congenital deficiency in IL-2, Bcl2 and Bim on differentiation and selection of T_{reg} and self-reactive effector T (T_{eff}) cells confounds interpretation of this observation. Antibody-mediated neutralization of IL-2 in thymectomized mice reduces T_{reg} cell numbers and Foxp3 expression in T_{reg} cells[16, 17]. Thus, IL-2 supports T_{reg} cell lineage stability after differentiation[18, 19]. However, expression of a transgene encoding IL-2Rβ chain exclusively in thymocytes was reported to rescue the lethal autoimmune disease in *Il2rb*$^{-/-}$ mice, suggesting that IL-2R expression is dispensable in peripheral T_{reg} cells[7, 11]. Thus, a role for IL-2R expression and signaling in peripheral T_{reg} cells remains uncertain. Hypothetically, a role for IL-2R in peripheral T_{reg} cells could be threefold: 1) guidance for T_{reg} cells to sense their targets – activated self-reactive T cells, which serve as a source of IL-2; 2) T_{reg} cell-mediated deprivation of IL-2 as a mechanism of suppression, and 3) cell-intrinsic IL-2 signaling in differentiated T_{reg} cells to support their maintenance, proliferation, or function due to triggering of JAK–STAT5, PI3K–Akt, or Ras–ERK signaling pathways. Previous studies primarily focused on the induction or maintenance of Foxp3, while other aspects of IL-2R function have not been firmly established due to aforementioned limitations.

Despite their high reliance on IL-2 for the maintenance of Foxp3 expression, T_{reg} cells are unable to produce IL-2. The reason for the inhibition of autologous activation of STAT5 in T_{reg} cells, and potential biological significance of this IL-2-based T_{reg}-T_{eff} cell regulatory loop, also remain unknown. It has been suggested that repression of IL-2 is required to maintain the 'unbound' state of high affinity IL-2R on T_{reg} cells, and unbound IL-2R serves a key role in T_{reg} cell-mediated suppression by depriving T_{eff} cells of IL-2[20-24], however, whether this mechanism has a non-redundant role in suppression *in vivo* is unknown.

To address the role of IL-2R and downstream signaling pathways in differentiated T_{reg} cells, we ablated IL-2Rα, IL-2Rβ, and STAT5 in Foxp3-expressing cells. By simultaneously

inducing expression of an active form of STAT5, we assessed the differential requirements for IL-2R expression and IL-2 signaling for T_{reg} cell homeostasis vs. suppressor activity.

Results

IL-2R is indispensable for T_{reg} cell function

To definitively establish a role for IL-2R in T_{reg} cell function *in vivo*, we generated a T_{reg} cell-specific IL-2Rβ conditional knockout mice using Cre recombinase driven by the endogenous *Foxp3* locus (*Foxp3*^{Cre}), in which a loxP-flanked *Il2rb* allele (*Il2rb*$^{fl/fl}$) was deleted in T_{reg} cells after Foxp3 was expressed. *Il2rb*$^{fl/fl}$*Foxp3*^{Cre} mice developed systemic fatal autoimmune inflammatory lesions and lymphoproliferation, albeit somewhat milder than that observed in *Foxp3*$^{-}$ mice (**Fig. 1a–c**). IL-2Rα expression was diminished in peripheral IL-2Rβ-deficient T_{reg} cells (**Fig. 1d**), and tyrosine phosphorylation of STAT5 in response to IL-2 was lacking (**Fig. 1e**). The frequency of Foxp3^{+} cells among CD4^{+} T cells and the expression of Foxp3 on a per-cell basis were both diminished (**Fig. 1f**). In healthy heterozygous *Il2rb*$^{fl/fl}$*Foxp3*$^{Cre/wt}$ females, where both IL-2Rβ-sufficient (YFP^{-}) and -deficient (YFP^{+}) T_{reg} cells co-exist due to random X-chromosome inactivation, IL-2Rβ-deficient T_{reg} cells were underrepresented (**Fig. 1g, h**). It has been suggested that IL-2 is selectively required for the maintenance of CD62L^{hi}CD44^{lo} Treg cells, but is dispensable for CD62L^{lo}CD44^{hi} T_{reg} cells[25]. However, we found both CD62L^{hi}CD44^{lo} and CD62L^{lo}CD44^{hi} T_{reg} cells to be significantly reduced in the absence of IL-2Rβ in healthy heterozygous females. In these mice, IL-2Rβ-deficient T_{reg} cells expressed reduced amounts of Foxp3 and T_{reg}-cell 'signature' molecules IL-2Rα chain (CD25), CTLA-4, GITR, and CD103 regardless of CD62L and CD44 expression (**Fig. 1i, j** and **Supplementary Fig. 1a**). Although in diseased *Il2rb*$^{fl/fl}$*Foxp3*^{Cre} mice, a majority of T_{reg} cells were CD62L^{lo}CD44^{hi}, this was likely a consequence of severe inflammation, because T_{reg} cell frequencies were also markedly reduced at sites where CD62L^{lo}CD44^{hi} cells were prevalent, i.e., the small and large intestines (**Supplementary Fig. 1b**). Accordingly, many characteristic T_{reg} cell markers, except for CD25 and Foxp3, were upregulated as the result of T_{reg} cell activation in *Il2rb*$^{fl/fl}$*Foxp3*^{Cre} mice (**Supplementary Fig. 1c**). These observations suggested that both CD62L^{hi}CD44^{lo} and CD62L^{lo}CD44^{hi} T_{reg} cell subsets, including those residing in the non-lymphoid tissues, are dependent on IL-2, though under inflammatory conditions the latter can be sustained to some extent by IL-2R-independent signals. Despite the upregulation of CTLA-4, GITR, ICOS, and CD103, the 'activated' IL-2Rβ-deficient T_{reg} cells from *Il2rb*$^{fl/fl}$*Foxp3*^{Cre} mice were still incapable of controlling inflammation in the diseased mice and were not suppressive when co-transferred with T_{eff} cells into lymphopenic recipients (data not shown).

Our findings raised the question whether ablation of IL-2Rα, which, in addition to facilitating IL-2 signaling, enables its sequestration from T_{eff} cells, would result in a similar T_{reg} cell deficiency and disease compared to those in *Il2rb*$^{fl/fl}$*Foxp3*^{Cre} mice. Thus, we generated a loxP-flanked *Il2ra* allele (J.D.F. manuscript in preparation) and similarly induced its conditional ablation in T_{reg} cells. We found that T_{reg} cell-specific IL-2Rα deficiency resulted in a disease with comparable early onset and severity to those observed upon IL-2Rβ ablation (**Supplementary Fig. 1d–f**). Of note, germ-line deficiency of either

Il2ra or *Il2rb* in mice on the same C57BL6/J as our conditional knockout mice resulted in a considerably less aggressive disease with a delayed onset, likely due to a role for IL-2R signaling in T_{eff} cells (data not shown). Our findings also indicate that IL-15 was unable to effectively compensate for the loss of IL-2 signaling in differentiated T_{reg} cells because in *Foxp3*^{Cre}*Il2ra*$^{fl/fl}$ mice, T_{reg} cells lacked only IL-2 signaling, whereas in *Il2rb*$^{fl/fl}$*Foxp3*^{Cre} mice, they lacked both IL-2 and IL-15 signaling yet were similarly affected. This was in contrast to T_{reg} cell differentiation in the thymus where IL-15 can contribute in part to Foxp3 induction[12]. Since IL-2R activates PI3K–Akt, MAPK, and JAK–STAT5 signaling pathways, we next sought to assess a role for STAT5 activation downstream of IL-2R signaling in T_{reg} cells. We found that STAT5 ablation similarly impaired T_{reg} cell function and *Foxp3*^{Cre}*Stat5a/b*$^{fl/fl}$ mice were similarly affected by fatal autoimmunity as were mice harboring IL-2R deficient T_{reg} cells (**Supplementary Fig. 1g–k).** Thus, in agreement with IL-2 neutralization studies, IL-2R signaling is required for T_{reg} cell fitness in a cell-intrinsic manner.

STAT5b-CA partially rescues IL-2R deficient T_{reg} function

The above findings implied that STAT5 activation downstream of IL-2R is continuously required for T_{reg} cell function. However, a marked decrease in IL-2R observed in STAT5-deficient T_{reg} cells (**Supplementary Fig. 1g**) made it impossible to separate a loss of STAT5 from impairment in all IL-2R functions, i.e., detection of IL-2, transduction of STAT5-dependent and -independent signals, and consumption and deprivation of IL-2, as a key contributor to the observed severe T_{reg} cell dysfunction.

To address this major caveat and to understand a role for STAT5 vs. IL-2R, we asked whether expression of a gain-of-function form of STAT5b can rescue T_{reg} cell function in the absence of IL-2R. A previous study using a transgene encoding a constitutively active form of STAT5b (STAT5b-CA) driven by the proximal *lck* promoter in the absence of IL-2Rβ showed rescue of T_{reg} cell differentiation in the thymus, but not lymphoproliferative syndrome[9]. However, the expression of this transgene early during thymopoiesis leads to leukemic lymphoproliferation, which complicated the interpretation of these findings. In addition, both the activity of the proximal *lck* promoter and the expression of the transgene diminish in peripheral T cells in these mice[9]. Therefore, we generated a gene-targeted mouse strain utilizing the *Rosa26* 'gene trap' locus[26], where a 'CAG' promoter driven STAT5b-CA[27] is preceded by a loxP-flanked STOP cassette (**Supplementary Fig. 2a**). In the resulting *Rosa26*^{Stat5bCA} mice, STAT5b-CA is expressed only when the loxP sites undergo Cre mediated recombination. Introduction of the *Rosa26*^{Stat5bCA} allele into *Il2rb*$^{fl/fl}$*Foxp3*^{Cre} mice and the consequent expression of STAT5b-CA in IL-2Rβ-deficient T_{reg} cells rescued the systemic inflammation and early fatal disease (**Supplementary Fig. 2b**). In these mice, T_{reg} cell frequencies and numbers were comparable to or even surpassed their levels in IL-2R sufficient *Foxp3*^{Cre} mice (**Fig. 2a**). Notably, the expression of IL-2Rα chain was increased despite the absence of IL-2Rβ chain (**Fig. 2a**), suggesting the expression of IL-2Rα on T_{reg} cells is primarily controlled by STAT5-dependent, but not by STAT5-independent signaling. Importantly, these IL-2Rβ-deficient T_{reg} cells with heightened IL-2Rα expression remained unresponsive to IL-2 (**Fig. 2b**).

The observed restoration of the suppressor function of IL-2Rβ-deficient T_{reg} cells and rescue of the early fatal disease upon STAT5b-CA expression raised the possibility that the reintroduced high IL-2Rα levels were responsible for these effects. However, the expression of STAT5b-CA similarly rescued the early fatal disease in *Foxp3*^{Cre}*Il2ra*$^{fl/fl}$ mice (**Supplementary Fig. 2c–h**). Importantly, although the impaired capacity of T_{reg} cells in both *Il2rb*$^{fl/fl}$*Foxp3*^{Cre} and *Foxp3*^{Cre}*Il2ra*$^{fl/fl}$ mice to capture and consume IL-2 was not rescued upon STAT5b-CA expression (**Fig. 2c**), CD4$^+$ T cell reactivity was fully controlled in these mice (**Fig. 2d** and **Supplementary Fig. 2d–h**). These results suggested that the ability to capture and compete for IL-2 is dispensable for T_{reg} cell mediated suppression of CD4$^+$ T cell responses. To the contrary, however, expansion of CD8$^+$ T cells, in particular, of activated CD62L^{hi}CD44^{hi} CD8$^+$ T cells, was only marginally restrained in these mice (**Fig. 2d** and **Supplementary Fig. 2f, h**). Although the expansion of CD8$^+$CD62L^{lo}CD44^{hi} subset was relatively well, albeit not perfectly, controlled in neonatal mice (**Fig. 2d** and **Supplementary Fig. 2f**), this subset also gradually started to expand in these mice as early as 3 wks after birth (**Supplementary Fig. 2i**). Although both *Il2rb*$^{fl/fl}$*Foxp3*^{Cre}*Rosa26*^{Stat5bCA} and *Il2ra*$^{fl/fl}$*Foxp3*^{Cre}*Rosa26*^{Stat5bCA} mice were rescued from premature death and showed significantly improved clinical status comparable to healthy controls, they gradually failed to thrive and started to succumb to disease accompanied by massively expanded activated CD62L^{hi}CD44^{hi} and CD62L^{lo}CD44^{hi} CD8$^+$ T cell subsets in LNs and tissues by approximately 12 wks of age (**Supplementary Fig. 2i, j**). These findings raised a possibility that IL-2 consumption by T_{reg} cells, while dispensable for control of CD4$^+$ T cells, is important for the restraint of CD8$^+$ T cells.

T_{reg} cells suppress CD8$^+$ T cell responses via IL-2 depletion

To test if the impairment in consumption of IL-2 by T_{reg} cells can account for the proliferation of CD8$^+$ T cells in *Foxp3*^{Cre}*Il2rb*$^{fl/fl}$*Rosa26*^{Stat5bCA} mice, we administered IL-2 neutralizing antibodies to these and control mice starting from 5–7 days of age (**Fig. 2e** and **Supplementary Fig. 3a**). As IL-2 supports the differentiation of T_{reg} cells in the thymus, IL-2 neutralization reduced the frequencies of T_{reg} cells in all groups of mice and induced immunoactivation in control *Il2rb*$^{fl/wt}$*Foxp3*^{Cre} mice. In *Il2rb*$^{fl/fl}$*Foxp3*^{Cre} mice, which spontaneously develop disease, the production of T_H2 cytokines IL-4 and IL-13 by CD4$^+$ T cells was significantly reduced by IL-2 neutralization; however, the activation of CD4$^+$ and CD8$^+$ T cells was at best only marginally reduced or unaffected. In contrast, the activation and proliferation of CD8$^+$ T cells observed in *Il2rb*$^{fl/fl}$*Foxp3*^{Cre}*Rosa26*^{Stat5bCA} mice were almost completely suppressed by the treatment.

The relative reduction in CD8$^+$CD62L^{lo}CD44^{hi} and more pronounced proliferation of CD8$^+$CD62L^{hi}CD44^{hi} T cell subset in *Il2rb*$^{fl/fl}$*Foxp3*^{Cre}*Rosa26*^{Stat5bCA} and *Il2ra*$^{fl/fl}$*Foxp3*^{Cre}*Rosa26*^{Stat5bCA} mice raised a possibility that a loss of IL-2-consumption by T_{reg} cells might selectively impair their suppression for memory CD8$^+$ T cell expansion, but not the recruitment of naive CD8$^+$ T cells into the effector cell pool. We tested this idea by adoptive transfer of CD4$^+$ and CD8$^+$ cell subsets into lymphopenic recipients (**Fig. 2f**). Consistent with the observation in *Foxp3*^{Cre} mice, the impaired suppression of CD4$^+$ T cell expansion and activation by IL-2R-deficient T_{reg} cells was completely rescued by STAT5b-CA; in contrast, their ability to suppress memory CD8$^+$ T cells was not restored, whereas

suppression of naive CD8$^+$ T cell expansion and expansion was only partially recovered. Thus, IL-2 consumption by T_{reg} cells appears to have a non-redundant role in suppressing the expansion and activation of both naive and memory CD8$^+$ T cell subsets, although this mechanism appears to be particularly prominent in control of the latter subset.

Although the majority of activated CD8$^+$ T cells in *Il2rb*$^{fl/fl}$*Foxp3*^{Cre} and *Il2rb*$^{fl/fl}$*Foxp3*^{Cre}*Rosa26*^{Stat5bCA} mice did not express detectable levels of IL-2Rα (**Supplementary Fig. 3a**), these cells could activate STAT5 in response to IL-2, albeit to a lesser extent than that observed in cells expressing IL-2Rα (**Supplementary Fig. 3b**). A small proportion of activated CD4$^+$ T cells with undetectable IL-2Rα expression also responded to IL-2, but the majority of them did not. CD8$^+$ T naive cells also responded to IL-2, while CD4$^+$ T naive cells did not. Thus, both naive and activated CD8$^+$ T cells appeared to be more sensitive to IL-2 than CD4$^+$ T cells, and IL-2 consumption by T_{reg} cells may markedly affect their activation. A corollary to this notion was that STAT5 activation in CD8$^+$, but not CD4$^+$ T cells may render the former resistant to T_{reg} cell mediated suppression. Thus, we tested the effect of STAT5 activation on the proliferation of CD4$^+$ and CD8$^+$ T cells in the presence of T_{reg} cells. For this purpose, we sorted CD4$^+$Foxp3$^-$ and CD8$^+$Foxp3$^-$ T cells from *Foxp3*^{Cre}*Rosa26*^{Stat5bCA} mice and induced the expression of STAT5b-CA in these cells by treating them with a recombinant Cre protein containing a membrane permeable TAT (trans-activating transcriptional activator from HIV virus) peptide (TAT-Cre). We adoptively transferred the treated cells into lymphopenic recipients with or without T_{reg} cells. Although TAT-Cre treatment initially induced STAT5b-CA expression in approximately 30% of the treated CD4$^+$ and CD8$^+$ T cells, more than 95% of CD8$^+$ T cells expressed STAT5b-CA three weeks after the transfer; whereas STAT5b-CA expressing CD4$^+$ T cells expanded to 40-50% (**Fig. 2g**). Notably, STAT5b-CA$^+$CD8$^+$ T cells robustly expanded in the presence of either control (*Foxp3*^{Cre}) or STAT5b-CA$^+$ T_{reg} cells (**Fig. 2g, h**). Although some degree of suppression of STAT5b-CA$^+$CD8$^+$ T cells by T_{reg} cells was still observed, it was very mild compared to the suppression of STAT5b-CA$^-$CD8$^+$ T cells (**Fig. 2h**). In contrast, proliferation of and cytokine production by activated CD4$^+$ T cells, regardless of the expression of STAT5b-CA, were well controlled by T_{reg} cells (**Fig. 2h**). These observations suggest that STAT5 activation in CD8$^+$, but not in CD4$^+$ T cells prompts robust expansion of cells and confers pronounced resistance to T_{reg} cell mediated suppression. Consistent with these findings, gain-of-function experiments where IL-2 was provided in the form of IL-2/ IL-2 immune complexes showed expansion of CD8$^+$ T and CD4$^+$ T_{reg}, but not of CD4$^+$ T cells[28]. Thus, while the ability to capture and compete for IL-2 is dispensable for T_{reg} cell mediated suppression of CD4$^+$ T cell responses, this mode of suppression appears essential for control of CD8$^+$ T cells, which respond to excessive IL-2 more robustly than CD4$^+$ T cells.

STAT5 activation in T_{reg}cells boosts immunosuppression

The lack of detectable STAT5 activation in response to IL-2 and of STAT5b-CA-driven expansion of IL-2R-sufficient T_{reg} cells that escaped from Cre-mediated recombination (counterselection) in both *Il2rb*$^{fl/fl}$*Foxp3*^{Cre}*Rosa26*^{Stat5bCA} and *Il2ra*$^{fl/fl}$*Foxp3*^{Cre}*Rosa26*^{Stat5bCA} mice indicated that the expression of an active form of STAT5 relieved T_{reg} cells from their dependence on IL-2 signaling. This finding offered a

unique opportunity to explore the biological significance of the aforementioned IL-2-dependent T_{reg}–T_{eff} cell regulatory network by uncoupling T_{reg} cell function from IL-2 production by T_{eff} cells. To address this question, we generated *Rosa26*^{Stat5bCA}*Foxp3*$^{Cre\text{-}ERT2}$ mice, which enabled tamoxifen-inducible expression of STAT5b-CA in differentiated T_{reg} cells[17]. Induction of STAT5b-CA expression in ~20–30% of T_{reg} cells upon a single tamoxifen administration was followed by their rapid increase in numbers at the expense of T_{reg} cells with a non-recombined *Rosa26*^{Stat5bCA} allele (**Supplementary Fig. 4a, b**). It is noteworthy that these cells exhibited a highly diverse TCR Vβ usage similar to that in control mice (**Supplementary Fig. 4c**).The experimental *Foxp3*$^{Cre\text{-}ERT2}$*Rosa26*^{Stat5bCA} mice remained healthy (**Supplementary Fig. 4d, e**). In these mice, the proliferated STAT5b-CA$^+$ T_{reg} cell population exhibited increased amounts of Foxp3, CD25, CTLA4, and GITR and an increased proportion of CD62L^{hi}CD44^{hi} vs. CD62L^{hi}CD44^{lo} cells, indicative of a STAT5b-CA impressed biasing of the T_{reg} cell population towards an activated or memory cell state (**Fig. 3a–d** and **Supplementary Fig. 4f**). Consistent with the latter possibility, surface expression of IL-7R, KLRG1, and CD103 were increased (**Fig. 3d**). Notably, in lymph nodes (LNs) and Peyer's patches (PPs), T_{reg} cells were not numerically increased despite the predominance of STAT5b-CA$^+$ T_{reg} cells (**Supplementary Fig. 4b, g**), suggesting that Treg cells with activated STAT5 preferentially distribute in non-lymphoid tissues. CD8$^+$Foxp3$^+$ cells were also increased upon induction of STAT5b-CA (**Supplementary Fig. 4h**). The 'autonomous' T_{reg} cells, expressing active STAT5 showed heightened *in vitro* suppressor activity (**Supplementary Fig. 4i**) and effectively suppressed the basal state of activation and proliferative activity of CD4$^+$ and CD8$^+$ T cells *in vivo,* as well, as evidenced by the decreased numbers of Ki-67$^+$ cells and CD62L^{lo}CD44^{hi} T_{eff} cells and a markedly increased CD62L^{hi}CD44^{lo} T naive cell pool (**Fig. 3e** and **Supplementary Fig. 5a, b**). Accordingly, CD4$^+$ T cell production of pro-inflammatory cytokines, most prominently IL-4, and expression of CD80 and CD86 by B cells and dendritic cells (DCs) were reduced (**Supplementary Fig. 5c** and **Fig. 3f**). These results indicate that expression of STAT5-CA confers increased suppressor function to T_{reg} cells. Previously, T_{reg} cells were proposed to promote systemic T_H17 type responses and IgA class switching in the gut[29, 30]. However, we found that serum and fecal IgA as well as T_H17 responses in secondary lymphoid organs were reduced, rather than increased in the presence of STAT5b-CA$^+$ T_{reg} cells (**Fig. 3g** and **Supplementary Fig. 5c**). Serum IgM and IgE also showed a tendency towards a decrease, but this was not statistically significant (**Supplementary Fig. 5d**). These results were in agreement with an increase in T_H17 responses and in both T_H2- and T_H1-type Ig class switch observed upon acute T_{reg} cell ablation[31]. Since altered intestinal immune responses have been implicated in promoting colonic carcinogenesis, we explored an effect of a gain in T_{reg} cell suppressor function afforded by activated STAT5 in an *Apc*^{Min} model of colorectal cancer. Mice harboring the *Apc*^{Min} mutation develop multiple adenomatous polyps in the small intestine[32]. *Apc*^{Min}*Foxp3*$^{Cre\text{-}ERT2}$*Rosa26*^{Stat5bCA} mice developed a comparable or fewer numbers of polyps, but the average polyp size was increased (**Supplementary Fig. 5e**). These results were consistent with the idea that suppression of inflammation by T_{reg} cells in tumor microenvironments promotes the growth of tumors once tumors or pre-cancerous lesions are already formed. However, the early stages of colonic carcinogenesis appeared not to be promoted but were potentially suppressed by T_{reg} cells with augmented suppressor activity.

In addition to restraining the basal immune reactivity in physiological settings and modulating colon carcinoma development, 'autonomous' T_{reg} cells afforded superior protection against autoantigen-induced autoimmunity. We found that *Foxp3*$^{Cre\text{-}ERT2}$*Rosa26*^{Stat5bCA} mice were highly resistant to experimental autoimmune encephalomyelitis (EAE) (**Fig. 4a–c**). The frequencies of $CD4^+Foxp3^+$ cells were significantly increased in the brain and spinal cord of these mice (**Fig. 4b**), and infiltration of inflammatory cells, including neutrophils and IL-17-producing $CD4^+$ T_H17 cells into these organs, was significantly reduced (**Fig. 4c**). Pathogen-specific responses were also diminished in *Foxp3*$^{Cre\text{-}ERT2}$*Rosa26*^{Stat5bCA} mice. Although Listeria-specific T_H1 responses were only modestly suppressed (**Fig. 4d**), vaccinia virus-specific $CD8^+$ T cell responses were markedly reduced in the presence of STAT5b-CA$^+$ T_{reg} cells (**Fig. 4e**). Our observation of diminished responses to infectious agents and modulation of cancer progression may provide a rationale as to why T_{reg} cells lack IL-2 production and autonomous activation of STAT5, and instead are reliant on activated T cells as a source of IL-2.

A distinct role for STAT5 activation in T_{reg} cells

Next, we sought to address the question of how sustained STAT5 signaling may potentiate T_{reg} cells' suppressive ability. In genetic loss- and gain-of-function studies, STAT5 activity in T_{reg} cells correlated with their proliferative capacity and expression of IL-2Rα and Foxp3. However, the *in vitro* suppression assays above, as well as the reduction in immune activation in LNs and PPs of *Foxp3*$^{Cre\text{-}ERT2}$*Rosa26*^{Stat5bCA} mice, where fewer T_{reg} cells were found than in control mice suggested that the enhanced immunosuppression observed in *Foxp3*$^{Cre\text{-}ERT2}$*Rosa26*^{Stat5bCA} mice was not simply due to a numerical increase of T_{reg} cells, but that their suppressor activity on a per cell basis was also augmented. It was also unlikely that mild upregulation of Foxp3 in the presence of STAT5b-CA could account for the increased suppressor activity of T_{reg} cells as we found that genome-wide Foxp3 binding does not change upon activation of T_{reg} cells, which lead to an increase in Foxp3 expression more pronounced than the one caused by STAT5b-CA[33]. The increase in Foxp3 protein in STAT5b-CA$^+$ T_{reg} cells compared to control was particularly noticeable in the $CD25^{lo}$ T_{reg} cell subset (**Fig. 3b**; Average fold changes in Foxp3 MFI in $Foxp3^+$ T_{reg} cells from *Foxp3*$^{Cre\text{-}ERT2}$*Rosa26*^{Stat5bCA} mice vs. those from *Foxp3*$^{Cre\text{-}ERT2}$ mice; $CD25^{hi}$ = 1.06 fold, $CD25^{lo}$ = 1.36 fold (n = 6)), consistent with the observation that STAT5b-CA$^+$ T_{reg} cells were relieved from their dependence on IL-2. Nevertheless, STAT5b-CA$^+$ T_{reg} cells exhibited a more potent suppressor function than $CD25^{hi}Foxp3^{hi}$ T_{reg} cells from control mice when co-transferred with T_{eff} cells into lymphopenic recipients despite comparably high expression of Foxp3 (data not shown). Thus, the increased suppressor activity of STAT5b-CA$^+$ T_{reg} cells was unlikely to be due to the increased Foxp3.

To gain insight into the potential mechanisms underlying the heightened suppressor function conferred by sustained STAT5 activation, we sorted mature T_{reg} cells from *Foxp3*$^{Cre\text{-}ERT2}$ and *Foxp3*$^{Cre\text{-}ERT2}$*Rosa26*^{Stat5bCA} mice that expressed comparable levels of Foxp3 and analyzed gene expression in these cells using RNA-seq. While the gene expression profiles of $CD4^+$ T naive cells from both groups of mice were nearly identical, T_{reg} cell gene expression was markedly affected by the active form of STAT5 (**Fig. 5a** and **Supplementary Fig. 6a**). Among all expressed genes (~11,000) in either T_{reg} or $CD4^+$ T naive cell

populations analyzed, 342 genes were upregulated and 314 genes were downregulated in STAT5b-CA$^+$ T_{reg} cells compared to control cells (**Fig. 5b** and **Supplementary Fig. 6b**). The gene set upregulated in STAT5b-CA$^+$ T_{reg} cells encoded various cell surface molecules and receptors involved in cell adhesion, migration, and cytoskeletal reorganization (**Fig. 5c**). Several genes that were upregulated or downregulated in control T_{reg} cells compared to T naive cells showed opposite trends in STAT5b-CA$^+$ T_{reg} cells, suggesting that STAT5b-CA does not simply reinforce the T_{reg} cell signature. A previous study showed that exposure of T_{reg} cells to inflammation induced upon transient T_{reg} cell depletion leads to a marked change in their gene expression and a potent increase in their suppressor function[33]. Consistent with the heightened suppressor function of STAT5b-CA$^+$ T_{reg} cells, we found that the gene expression changes in these cells conferred by an active form of STAT5 correlated with those found in highly activated T_{reg} cells in inflammatory settings (**Fig. 5d**). TCR signaling is required for the ability of T_{reg} cells to exert their suppressor function[34, 35]. Thus, it was possible that TCR and STAT5 dependent signaling pathways in T_{reg} cells are acting upon a largely overlapping set of genes whose expression they jointly regulate to potentiate T_{reg} cell suppressor activity. However, our analysis revealed that the gene set affected by the active form of STAT5 was distinct from that expressed in T_{reg} cells in a TCR-dependent manner (**Fig. 5d**). Thus, both TCR and STAT5 signaling pathways play an indispensable role in T_{reg} cell suppressor activity *in vivo* by controlling largely distinct sets of genes and likely distinct aspects of T_{reg} cell suppressor activity.

To better understand aspects of T_{reg} cell function potentiated by STAT5 activation, we performed signaling pathway and molecular function enrichment analyses, which revealed overrepresentation of gene sets involved in cell-cell and extracellular matrix interactions, cell adhesion, and cellular locomotion among genes differentially expressed in STAT5b-CA$^+$ T_{reg} cells (**Fig. 5e, f, Supplementary Fig. 6c**). This result suggested that in T_{reg} cells, STAT5 activation might potentiate their interactions with the target cells. Since intravital imaging of T_{reg} cells *in vivo* had previously revealed their stable interactions with DCs[36], we assessed the potential effect of constitutively active STAT5 expression in T_{reg} cells on their ability to form conjugates with DCs *in vitro*. In agreement with the gene set enrichment analysis, we found that STAT5b-CA expression in Treg cells promotes conjugate formation between T_{reg} and DCs (**Fig. 6a**). Heightened interactions of STAT5b-CA$^+$ T_{reg} cells with DCs *in vitro* were consistent with the decreased expression of co-stimulatory molecules by DCs observed in tamoxifen-treated *Foxp3*$^{Cre\text{-}ERT2}$*Rosa26*^{Stat5bCA} mice.

These findings raised a question whether STAT5 activation can potentiate the suppressor function of T_{reg} cells in a TCR-independent manner. To test this notion, we analyzed *Foxp3*$^{Cre\text{-}ERT2}$*Rosa26*^{Stat5bCA} mice expressing a conditional *Tcra* allele. As we reported previously, tamoxifen-inducible Cre-mediated TCR ablation in T_{reg} cells is highly efficient in these mice and resulted in immune activation resulting from impaired suppressor function[34]. In heterozygous *Foxp3*$^{Cre\text{-}ERT2}$*Tcra*$^{fl/wt}$ mice, Cre mediated recombination can theoretically result in ablation of TCR in up to a half of T_{reg} cells due to the allelic exclusion at the *Tcra* locus. We observed a small proportion of TCR-deficient T_{reg} cells after 2-wks of tamoxifen administration in these mice (**Fig. 6b**). Although the expression of the active form of STAT5 was observed in ~50% of TCR-sufficient and -deficient T_{reg} cells in

Foxp3$^{Cre\text{-}ERT2}$ *Tcra*$^{fl/wt}$ *Rosa26*^{Stat5bCA} mice, the proportion of only TCR-sufficient, but not -deficient STAT5b-CA expressing T_{reg} cells was increased. The marked increase in T cell activation and pro-inflammatory cytokine production was mitigated in part upon expression of the active form of STAT5 in tamoxifen-treated *Foxp3*$^{Cre\text{-}ERT2}$ *Tcra*$^{fl/fl}$ *Rosa26*^{Stat5bCA} mice (**Fig. 6c**). This partial recovery of T_{reg} cell suppressor function by the active form of STAT5 in TCR-ablated T_{reg} cells was also confirmed in experiments where flow-sorted TCR-deficient STAT5b-CA$^+$ T_{reg} cells and T_{eff} cells were adoptively transferred into lymphopenic recipients (**Fig. 6d**). Although the rescue was incomplete, these results suggested that enhanced STAT5 signaling could potentiate T_{reg} cell suppressor activity in the absence of contemporaneous TCR-dependent signals. Indeed, some features of T_{reg} cells that had been observed in TCR-sufficient STAT5b-CA$^+$ T_{reg} cells were still present in TCR-ablated STAT5b-CA$^+$ T_{reg} cells (**Fig. 6c, d**). It should be noted, however, that STAT5b-CA expression failed to rescue suppressor function in *Foxp3*^{Cre} *Tcra*$^{fl/fl}$ *Rosa26*^{Stat5bCA} mice where TCR deletion occurred immediately after the induction of Foxp3. It was previously shown that TCR signaling is required for T_{reg} cells to acquire an activated, antigen-experienced phenotype and suppressor function[34]. Thus, our results suggest that activation of STAT5 potentiates TCR-independent suppressor function in mature T_{reg} cells that have already undergone TCR-dependent maturation. This observation is reminiscent of the sequential requirement for these two signals, TCR and IL-2R, in the differentiation of T_{reg} cells in the thymus where STAT5 signal promotes differentiation of T_{reg} precursors that have experienced permissive TCR signaling[37].

Discussion

Previous analysis of mice with germ-line deficiency in IL-2 and IL-2R subunits demonstrated that IL-2 is a key cytokine required for the induction of Foxp3 and the differentiation of T_{reg} cells in the thymus[5-11] . Furthermore, antibody-mediated IL-2 neutralization and provision of IL-2-complexes, as well as genetic dissection of regulatory elements within the Foxp3 locus, revealed an important role for IL-2 in the maintenance of mature T_{reg} cells and in stabilization of Foxp3 expression during their extrathymic differentiation[16, 28, 38]. These findings raised a question of whether IL-2R signaling can also directly promote T_{reg} cell suppressor capacity and, therefore, serve as a critical nexus linking differentiation and maintenance of T_{reg} cells with their suppressor function. An early *in vitro* study proposed a role for IL-2 signaling based on indirect evidence[21]. In addition, IL-2 consumption by T_{reg} cells was suggested to play an essential role in T_{reg} cell suppressor function by causing death of activated CD4$^+$ T cells due to IL-2 deprivation[20-24]. On the other hand, other reports suggested that IL-2R is dispensable for the ability of T_{reg} cells to suppress effector T cell proliferation[8, 39]. Furthermore, the rescue of the disease in *Il2ra*$^{-/-}$ and *Il2rb*$^{-/-}$ mice observed upon adoptive transfer of wild-type T_{reg} cells suggested the existence of major mechanisms of T_{reg} cell-mediated suppression independent of IL-2-deprivation[6, 7]. However, the latter studies left open a major question as to whether IL-2 consumption by T_{reg} cells is essential for suppression of IL-2R-sufficient T_{eff} cells since IL-2 is likely a major driver of autoimmune disease in the absence of functional T_{reg} cells.

A major limiting factor in efforts to experimentally assess a role for IL-2R signaling in, and IL-2 consumption by T_{reg} cells in their function *in vivo* has been the lack of adequate

genetic tools. We addressed this issue through generation of conditional *Il2ra* and *Il2rb* alleles and their ablation in T_{reg} cells in combination with the induced expression of an active form of STAT5. These new genetic tools enabled us to unequivocally demonstrate that IL-2R signaling has a cell intrinsic, non-redundant role not only in the maintenance of mature T_{reg} cells and their fitness, but also in their suppressor function. Furthermore, we found that STAT5 deficiency in T_{reg} cells results in a similar loss of suppressor function and that expression of an active form of STAT5 can rescue fatal disease resulting from IL-2R deficiency. These results suggest a key role of IL-2R–STAT5 signaling in linking differentiation and maintenance of T_{reg} cells and their function. STAT5 binds to the *Foxp3* promoter and the intronic *Foxp3* regulatory element CNS2 and is involved in Foxp3 induction and maintenance[38]. Runx-CBFβ complexes also bind to CNS2 and the Foxp3 promoter and affect Foxp3 expression levels[40]. Although both CNS2- and CBFβ-deficient T_{reg} cells do exhibit reduced Foxp3 expression resembling that of STAT5- or IL-2R-deficient T_{reg} cells, the impairment of suppressor function in the latter was much more severe. Thus, the decrease in Foxp3 expression alone cannot account for a severe loss of T_{reg} cell suppressor function in the absence of STAT5 or IL-2R. Indeed, our analysis of gene expression and functional features conferred upon expression of the active form of STAT5 pointed to a heightened ability of T_{reg} cells to bind to DC and suppress their activation. Furthermore, expression of an active form of STAT5 partially rescued the near-complete loss of T_{reg} suppressor function in the absence of TCR signaling[34, 35]. These results may appear at odds with the previous finding that STAT5b-CA transgene driven by the proximal *lck* promoter and Eμenhancer failed to curtail fatal lymphoproliferative disease in *Il2rb*$^{-/-}$ mice despite restoring Foxp3 expression and T_{reg} cell differentiation in the thymus[9]. However, the interpretation of the latter result is problematic due to a massive expansion of pre-leukemic T and B cells and reduced expression of the STAT5b-CA transgene in peripheral T_{reg} cells.

Our studies clearly demonstrated that IL-2-deprivation by T_{reg} cells was fully dispensable for suppression of IL-2R-sufficient $CD4^+$ T cells even though IL-2R signaling was required. However, IL-2R dependent IL-2 consumption by T_{reg} cells was indispensable for suppression of $CD8^+$ T cell responses. The latter seemingly unexpected finding makes sense in light of the observed exquisite sensitivity of both naive and activated $CD8^+$ T cells to IL-2 induced stimulation. Furthermore, IL-2 is produced upon activation of both naive $CD4^+$ and $CD8^+$ T cells within hours after TCR engagement in contrast to effector cytokines such as IL-4 and IFN-γ whose production requires T naive cell differentiation into T_{eff} cells on a much longer time scale[41]. These distinguishing features provide a likely explanation for a need for a distinct mechanism of control of $CD8^+$ T cell responses by T_{reg} cells through IL-2 consumption.

It has been suggested that sensing of local IL-2 production by T_{reg} cells enables 'licensing' of their suppressor function[21]. However, the rescue of suppression of $CD4^+$ T cell responses by IL-2R-deficient T_{reg} cells expressing an active form of STAT5 suggests that activated T_{reg} cells can suppress autoimmunity without identifying the cellular source of IL-2. Thus, while IL-2 is a booster for T_{reg} cell suppressor function, it may not play an indispensable role as a cue for specific targeting.

Genetically modified T cells are emerging as a potent means of therapy in some forms of cancer. The observed enhanced suppressor activity of T_{reg} cells expressing an active form of STAT5 and significantly reduced severity of organ-specific autoimmunity in their presence suggest that such a modification of T_{reg} cells may hold promise for an optimal design of T_{reg} cell-based therapies for a variety of autoimmune and inflammatory disorders and in organ transplantation.

Our findings highlight the central role of IL-2 receptor signaling driven STAT5 activation in supporting and boosting suppressor function of differentiated T_{reg} cells. In this regard, it is noteworthy that although a *Foxp3* ortholog has not been identified in birds, chicken and duck $CD4^+$ T cell subsets expressing high amounts of IL-2Rα chain possess *in vitro* suppressor activity suggesting the importance of evolutionary conservation of IL-2Rα function in suppressive T cells[42, 43].

Methods

Mice

Foxp3^{Cre} and *Foxp3*$^{Cre\text{-}ERT2}$ mice were described previously[17, 44]. *Il2ra*^{fl} mice were generated by J.D.F. *Stat5a/b*^{fl} mice were provided by L Henninghausen. *Apc*^{Min} mice were purchased from the Jackson Laboratory. The targeting strategies to generate *Il2rb*^{fl} (generated by U.K.) and *Rosa26*^{Stat5bCA} alleles are shown in **Supplementary Fig. 7**. *Tcra*^{fl} mice were described previously[34]. The experimental mice were either generated on or backcrossed onto a C57BL/6J (B6) background, bred and housed in the specific pathogen-free animal facility at Memorial Sloan Kettering Cancer Center (MSKCC). All animal experiments were approved by institutional animal care and use committee at MSKCC and were performed in accordance with the institutional guidelines. For survival analysis, mice were monitored daily and unhealthy mice were euthanized once they are found lethargic and counted as non-survivors. For tamoxifen treatment, tamoxifen (Sigma-Aldrich) was dissolved in olive oil at a concentration of 40 mg/ml. Mice were given oral gavage of 100 μl of tamoxifen emulsion per treatment. In EAE and infection experiments, mice were challenged 2 to 3 months after a single tamoxifen gavage and assessed as described previously[38].

Flow cytometry and cell sorting

Cells were stained with fluorescently tagged antibodies purchased from eBioscience, BD Biosciences, Tonbo Bioscience, or BioLegend (**Supplementary Table 2**) and analyzed using a BD LSR II flow cytometer. Flow cytometry data were analyzed using FlowJo software (TreeStar). For intracellular cytokine staining, cells were stimulated for 5 hr with CD3 and CD28 antibodies (5 μg/ml each) in the presence of brefeldin A or monensin, harvested and stained with eBioscience Fixation Permeabilization kit. For intracellular phosphorylated STAT5 staining, cells were stimulated with or without rmIL-2 for 20 min, fixed and permeabilized with 4% PFA followed by 90% methanol, and stained with anti-pY-STAT5 antibody (BD Biosciences). Cell sorting of $Foxp3^+$ and $Foxp3^-$ cells was performed based on YFP or GFP expression using a BD FACSAria II cell sorter.

Listeria and *Vaccinia* infection

Mice were intravenously injected into the tail vein with *Listeria monocytogenes* (LM10403S; 2000 cells/mouse) on day 0 and analyzed on day 8. For the detection of *Listeria*-specific immune responses, splenic DCs from unchallenged B6 mice sorted using CD11c microbeads (Miltenyi) were cultured in wells of a 96 well U-bottom plate (2×10^4 cells/well) with heat-killed *Listeria monocytogenes* (2×10^7 cells/well) for 6 hr prior to the analysis. The cells were then co-cultured with splenic T cells obtained from *Listeria*-infected mice (1×10^5 cells/well) for 5 hr in the presence of brefeldin A, and cytokine producing T cells were detected by flow cytometry. For vaccinia virus infection, mice were intraperitoneally injected with non-replicating virus (5×10^7 PFU/mouse) on day 0 and analyzed on day 8. Splenocytes were re-stimulated with several vaccinia virus derived antigenic peptides (1 μg/ml) for 5 hr in the presence of brefeldin A, and cytokine producing T cells were detected by flow cytometry.

In vivo IL-2 neutralization

Mice were i.p. injected with a cocktail of two different anti-IL-2 monoclonal antibodies JES6-1 and S4B6-1 (BioXcell) or isotype matched control antibody (rat IgG2a, 2A3; BioXcell), 200 μg each, twice a week, starting from 5–7 days after birth.

TAT-Cre protein treatment of T cells

For the induction of STAT5b-CA expression in non-T_{reg} cells, 1×10^7 $CD4^+Foxp3^-$ or $CD8^+Foxp3^-$ T cells sorted from the LNs and spleens of *Foxp3*^{Cre} and *Foxp3*^{Cre}*Rosa26*^{Stat5bCA} mice were resuspended in 2 ml of serum-free RPMI media containing a TAT-Cre recombinase (Millipore; 50 μg/ml) and incubated at 37°C for 45 min. The cells were washed with RPMI containing 10% FCS, resuspended in PBS, and injected into T cell-deficient (*Tcrb*$^{-/-}$ *Tcrd*$^{-/-}$) mice together with or without separately sorted T_{reg} cells for *in vivo* suppression assay.

In vitro IL-2 capture assay

Pooled cells from LNs and spleens were depleted of B cells and accessary cells by panning and T cells were enriched. The cells were stained with anti-CD8 and anti-B220 Abs, and $CD4^+$ T_{reg} cells were sorted on the basis of GFP (YFP) expression alone in CD8-negative population. The sorted cells were divided among 8 wells of a 96-well V-bottomed plate (2×10^5 cells/well) in 25 μl RPMI medium (10% FCS) with or without increasing doses of recombinant human IL-2 (0.016 to 12 U/ml), followed by incubation for 2 h at 37 °C. Depletion of IL-2 from the medium was assessed with the BD Cytometric Bead Array and Human IL-2 Enhanced Sensitivity Flex Set according to the manufacturer's instructions (BD Biosciences).

In vitro T–DC conjugation assay

T_{reg} cells and non-T_{reg} cells were sorted in the same manner as IL-2 capture assay. Splenic $CD11c^+$ DCs were isolated by MACS from B6 mice injected with Flt3L-secreting B16 melanoma cells. T_{reg} and non-T_{reg} cells were stained with CFSE. DCs were stained with CellTrace Violet (Molecular Probes). 1×10^4 T_{reg} or non-T_{reg} cells were cultured together

with graded numbers of DCs (1×10^4 to 1×10^5) in a 96-well round-bottomed plate for 720 min in the presence or absence of rmIL-2 (100 IU/ml). Frequencies of T_{reg} cells conjugated with DCs (% $CTV^+CFSE^+/CFSE^+$) were analyzed by flow cytometry.

In vitro suppression assay

Naive $CD4^+$ T cells (responder cells) and T_{reg} cells were FACS purified and stained with CellTrace Violet (CTV). 4×10^4 naive $CD4^+$ T cells were cultured with graded numbers of T_{reg} cells in the presence of 1×10^5 irradiated, T-cell-depleted, CFSE-stained splenocytes and 1 μg/ml anti-CD3 antibody in a 96 round-bottom plate for 80 hr. Cell proliferation of responder T cells and T_{reg} cells (live $CFSE^-CD4^+Foxp3^-$ and $Foxp3^+$) was determined by flow cytometry based on the dilution of fluorescence intensity of CTV of the gated cells.

Measurements of serum and fecal immunoglobulin levels

Serum IgM, IgG1, IgG2a, IgG2b, IgG2c, IgG3 and IgA levels were determined by ELISA using SBA Clonotyping System (Southern Biotech). IgE ELISA was performed using biotinylated anti-IgE antibody (BD Biosciences) and HRP-conjugated streptavidin. For measurement of fecal IgA levels, fresh fecal pellets were collected and dissolved in extraction buffer (7 μl per mg pellet) containing 50 mM Tris-HCl, 150 mM NaCl, 0.5% NP-40, 1mM EDTA, 1 mM DTT, and protease inhibitor cocktail (Complete mini; Roche). Supernatants were collected after centrifugation, titrated, and IgA levels were measured by ELISA.

Statistical Analysis for Animal Experiments

Each mouse was tagged with a unique identification number, and researchers were blinded to the genotypes of mice except for adjusting sample size included in a single experiment and after data analysis is completed. Wild type mice with suspected congenital anomalies were excluded from the study. Cell samples that showed less than 70% cell vitality after preparation or after *in vitro* stimulation were excluded from the study. Statistical analyses were performed using Prism software with two-tailed unpaired Student's t test. Welch's correction was applied when F test was positive. P values < 0.05 were considered significant.

RNA sequencing

Male 8-wk-old *Foxp3*$^{Cre\text{-}ERT2}$*Rosa26*^{Stat5bCA} (STAT5b-CA) and *Foxp3*$^{Cre\text{-}ERT2}$ (control) mice, nine mice for each experimental group, received a single dose (4 mg) of tamoxifen by oral gavage 4 months before isolation. Splenic $CD4^+Foxp3(YFP/GFP)^+GITR^{hi}CD25^{hi}$ T_{reg} and $CD4^+Foxp3(YFP/GFP)^-CD62L^{hi}CD44^{lo}$ naive T cells were double sorted using a BD FACSAria II cell sorter, and a total of 12 samples were generated. Spleen T cell subsets isolated from three individual mice in the same experimental group were pooled into one biological replicate; three biological replicates were subjected to RNA-seq analysis for each experimental group. Total RNA was extracted and used for poly(A) selection and Illumina TruSeq paired-end library preparation following manufacturer's protocols. Samples were sequenced on the Illumina HiSeq 2500 to an average depth of 27.5 million 50-bp read pairs

per sample. All samples were processed at a same time and sequenced on the same lane to avoid batch effects.

Read alignment and processing followed the method previously described[45]. Briefly, raw reads were trimmed using Trimmomatic v0.32 with standard settings to remove low-quality reads and adaptor contamination[46]. The trimmed reads were then aligned to the mouse genome (Ensembl assembly GRCm38) using TopHat2 v2.0.11 implementing Bowtie2 v2.2.2 with default settings. Read alignments were sorted with SAMtools v0.1.19 before being counted to genomic features using HTSeq v0.6.1p1. The overall read alignment rate across all samples was 74.5%. Differential gene expression was analyzed using DESeq2 1.6.3 in R version 3.1.0[47].

Bioinformatic analyses for RNA-seq

The distribution of read counts across all genes was bimodal. The assumption that this corresponded to "expressed" and "non-expressed" genes was supported by examination of marker genes known to be expressed or not expressed in T_{reg} and T naive cells. The local minimum between the two peaks was chosen to be the threshold for expression. Using this threshold of ~60 normalized reads, 10,589 out of 39,179 genes were called as present. Significantly up- (342 genes) and down-regulated (314) genes between STAT5b-CA versus control T_{reg} cells were defined as expressed genes with fold changes of at least 1.5× or 0.67×, respectively, and FDR-adjusted *P*-value ≤0.05.

TCR-upregulated (i.e., TCR-dependent) genes were defined as genes downregulated (at least 0.57× fold change) in TCR-deficient compared to TCR-sufficient $CD44^{hi}$ T_{reg} cells, while TCR-downregulated genes are upregulated (at least 1.75×, P_{adj} ≤0.001) in TCR-deficient $CD44^{hi}$ T_{reg} cells (GSE61077)[34]. Activation-upregulated genes are genes upregulated (2× fold change, P_{adj} ≤0.01) in T_{reg} cells from *Foxp3*^{DTR} mice recovering from punctual T_{reg} cell depletion (GSE55753)[33].

Signaling Pathway Impact Analysis (SPIA) was performed using the R package of the same name[48]. Significantly up- and downregulated genes, and their fold changes, were analyzed as one set for enrichment and perturbation of 90 *Mus musculus* KEGG pathways accessed on October 5, 2015. The net pathway perturbation Z-score was calculated using the observed net perturbation accumulation, and the mean and SD of the null distribution of net perturbation accumulations. Global *P*-values were calculated using the normal inversion method with Bonferroni correction.

Biological process (BP) gene ontology (GO) term over-representation was calculated using BiNGO v3.0.3[49] in Cytoscape v3.2.1, employing the hypergeometric test and applying a significance cutoff of FDR-adjusted *P*-value ≤0.05. The 10,589 expressed genes were entered as the reference set, and the GO ontology and annotation files used were downloaded on Oct. 25, 2015 (**Supplementary Table 1**). The output from BiNGO was imported into EnrichmentMap v2.0.1[50] in Cytoscape to cluster redundant GO terms and visualize the results. An EnrichmentMap was generated using a Jaccard similarity coefficient cutoff of 0.2, a *P*-value cutoff of 0.001, an FDR-adjusted cutoff of 0.005, and

excluding gene sets with fewer than 10 genes. The network was visualized using a prefuse force-directed layout with default settings and 500 iterations. Groups of similar GO terms were manually circled.

Supplementary Material

Refer to Web version on PubMed Central for supplementary material.

Acknowledgments

We thank T. Kitamura (The University of Tokyo) for mSTAT5b-CA vector (pMX-STAT5B(1*6)) and K. Rajewsky (Max Delbrück Center) for *Rosa26* construct, L. Henninghausen (NIH) for *Stat5a/b* conditional allele. Supported by the Japan Society for the Promotion of Science, Strategic Young Researcher Overseas Visits Program for Accelerating Brain Circulation (T.C.), Lucille Castori Center for Microbes, Inflammation & Cancer (T.C.), NIH Medical Scientist Training Program grant T32GM07739 to the Weill Cornell/Rockefeller/Sloan Kettering Tri-Institutional MD-PhD Program (A.G.L. and X.F.), the US National Institutes of Health (P30 CA008748 to MSKCC Core Facilities, R37 AI034206 to A.Y.R.), the Ludwig Center at Memorial Sloan Kettering Cancer Center (A.Y.R.), Hilton-Ludwig Cancer Prevention Initiative funded by the Conrad N. Hilton Foundation and Ludwig Cancer Research (A.Y.R.), and the Howard Hughes Medical Institute (A.Y.R.).

References

1. Sakaguchi S, Sakaguchi N, Asano M, Itoh M, Toda M. Immunologic self-tolerance maintained by activated T cells expressing IL-2 receptor alpha-chains (CD25). Breakdown of a single mechanism of self-tolerance causes various autoimmune diseases. J Immunol. 1995; 155:1151–1164. [PubMed: 7636184]
2. Hori S, Nomura T, Sakaguchi S. Control of regulatory T cell development by the transcription factor Foxp3. Science. 2003; 299:1057–1061. [PubMed: 12522256]
3. Fontenot JD, Gavin MA, Rudensky AY. Foxp3 programs the development and function of CD4+CD25+ regulatory T cells. Nature immunology. 2003; 4:330–336. [PubMed: 12612578]
4. Waldmann TA. The multi-subunit interleukin-2 receptor. Annual review of biochemistry. 1989; 58:875–911.
5. Furtado GC, Curotto de Lafaille MA, Kutchukhidze N, Lafaille JJ. Interleukin 2 signaling is required for CD4(+) regulatory T cell function. The Journal of experimental medicine. 2002; 196:851–857. [PubMed: 12235217]
6. Almeida AR, Legrand N, Papiernik M, Freitas AA. Homeostasis of peripheral CD4+ T cells: IL-2R alpha and IL-2 shape a population of regulatory cells that controls CD4+ T cell numbers. J Immunol. 2002; 169:4850–4860. [PubMed: 12391195]
7. Malek TR, Yu A, Vincek V, Scibelli P, Kong L. CD4 regulatory T cells prevent lethal autoimmunity in IL-2Rbeta-deficient mice. Implications for the nonredundant function of IL-2. Immunity. 2002; 17:167–178. [PubMed: 12196288]
8. Fontenot JD, Rasmussen JP, Gavin MA, Rudensky AY. A function for interleukin 2 in Foxp3-expressing regulatory T cells. Nature immunology. 2005; 6:1142–1151. [PubMed: 16227984]
9. Burchill MA, Yang J, Vogtenhuber C, Blazar BR, Farrar MA. IL-2 receptor beta-dependent STAT5 activation is required for the development of Foxp3+ regulatory T cells. J Immunol. 2007; 178:280–290. [PubMed: 17182565]
10. Yao Z, et al. Nonredundant roles for Stat5a/b in directly regulating Foxp3. Blood. 2007; 109:4368–4375. [PubMed: 17227828]
11. Malek TR, Bayer AL. Tolerance, not immunity, crucially depends on IL-2. Nature reviews. Immunology. 2004; 4:665–674.
12. Vang KB, et al. IL-2, -7, and -15, but not thymic stromal lymphopoeitin, redundantly govern CD4+Foxp3+ regulatory T cell development. J Immunol. 2008; 181:3285–3290. [PubMed: 18714000]

13. Chen W, et al. Conversion of peripheral CD4+CD25− naive T cells to CD4+CD25+ regulatory T cells by TGF-beta induction of transcription factor Foxp3. The Journal of experimental medicine. 2003; 198:1875–1886. [PubMed: 14676299]
14. Malin S, et al. Role of STAT5 in controlling cell survival and immunoglobulin gene recombination during pro-B cell development. Nature immunology. 2010; 11:171–179. [PubMed: 19946273]
15. Barron L, et al. Cutting edge: mechanisms of IL-2-dependent maintenance of functional regulatory T cells. J Immunol. 2010; 185:6426–6430. [PubMed: 21037099]
16. Setoguchi R, Hori S, Takahashi T, Sakaguchi S. Homeostatic maintenance of natural Foxp3(+) CD25(+) CD4(+) regulatory T cells by interleukin (IL)-2 and induction of autoimmune disease by IL-2 neutralization. The Journal of experimental medicine. 2005; 201:723–735. [PubMed: 15753206]
17. Rubtsov YP, et al. Stability of the regulatory T cell lineage in vivo. Science. 2010; 329:1667–1671. [PubMed: 20929851]
18. Komatsu N, et al. Heterogeneity of natural Foxp3+ T cells: a committed regulatory T-cell lineage and an uncommitted minor population retaining plasticity. Proceedings of the National Academy of Sciences of the United States of America. 2009; 106:1903–1908. [PubMed: 19174509]
19. Hori S. Lineage stability and phenotypic plasticity of Foxp3(+) regulatory T cells. Immunological reviews. 2014; 259:159–172. [PubMed: 24712465]
20. Pandiyan P, Zheng L, Ishihara S, Reed J, Lenardo MJ. CD4+CD25+Foxp3+ regulatory T cells induce cytokine deprivation-mediated apoptosis of effector CD4+ T cells. Nature immunology. 2007; 8:1353–1362. [PubMed: 17982458]
21. Thornton AM, Donovan EE, Piccirillo CA, Shevach EM. Cutting edge: IL-2 is critically required for the in vitro activation of CD4+CD25+ T cell suppressor function. J Immunol. 2004; 172:6519–6523. [PubMed: 15153463]
22. Barthlott T, et al. CD25+ CD4+ T cells compete with naive CD4+ T cells for IL-2 and exploit it for the induction of IL-10 production. International immunology. 2005; 17:279–288. [PubMed: 15684039]
23. Busse D, et al. Competing feedback loops shape IL-2 signaling between helper and regulatory T lymphocytes in cellular microenvironments. Proceedings of the National Academy of Sciences of the United States of America. 2010; 107:3058–3063. [PubMed: 20133667]
24. Yamaguchi T, et al. Construction of self-recognizing regulatory T cells from conventional T cells by controlling CTLA-4 and IL-2 expression. Proceedings of the National Academy of Sciences of the United States of America. 2013; 110:E2116–2125. [PubMed: 23690575]
25. Smigiel KS, et al. CCR7 provides localized access to IL-2 and defines homeostatically distinct regulatory T cell subsets. The Journal of experimental medicine. 2014; 211:121–136. [PubMed: 24378538]
26. Zambrowicz BP, et al. Disruption of overlapping transcripts in the ROSA beta geo 26 gene trap strain leads to widespread expression of beta-galactosidase in mouse embryos and hematopoietic cells. Proceedings of the National Academy of Sciences of the United States of America. 1997; 94:3789–3794. [PubMed: 9108056]
27. Onishi M, et al. Identification and characterization of a constitutively active STAT5 mutant that promotes cell proliferation. Molecular and cellular biology. 1998; 18:3871–3879. [PubMed: 9632771]
28. Boyman O, Kovar M, Rubinstein MP, Surh CD, Sprent J. Selective stimulation of T cell subsets with antibody-cytokine immune complexes. Science. 2006; 311:1924–1927. [PubMed: 16484453]
29. Chen Y, et al. Foxp3(+) regulatory T cells promote T helper 17 cell development in vivo through regulation of interleukin-2. Immunity. 2011; 34:409–421. [PubMed: 21435588]
30. Cong Y, Feng T, Fujihashi K, Schoeb TR, Elson CO. A dominant, coordinated T regulatory cell-IgA response to the intestinal microbiota. Proceedings of the National Academy of Sciences of the United States of America. 2009; 106:19256–19261. [PubMed: 19889972]
31. Kim JM, Rasmussen JP, Rudensky AY. Regulatory T cells prevent catastrophic autoimmunity throughout the lifespan of mice. Nature immunology. 2007; 8:191–197. [PubMed: 17136045]
32. Su LK, et al. Multiple intestinal neoplasia caused by a mutation in the murine homolog of the APC gene. Science. 1992; 256:668–670. [PubMed: 1350108]

33. Arvey A, et al. Inflammation-induced repression of chromatin bound by the transcription factor Foxp3 in regulatory T cells. Nature immunology. 2014; 15:580–587. [PubMed: 24728351]
34. Levine AG, Arvey A, Jin W, Rudensky AY. Continuous requirement for the TCR in regulatory T cell function. Nature immunology. 2014; 15:1070–1078. [PubMed: 25263123]
35. Vahl JC, et al. Continuous T cell receptor signals maintain a functional regulatory T cell pool. Immunity. 2014; 41:722–736. [PubMed: 25464853]
36. Tadokoro CE, et al. Regulatory T cells inhibit stable contacts between CD4+ T cells and dendritic cells in vivo. The Journal of experimental medicine. 2006; 203:505–511. [PubMed: 16533880]
37. Lio CW, Hsieh CS. A two-step process for thymic regulatory T cell development. Immunity. 2008; 28:100–111. [PubMed: 18199417]
38. Feng Y, et al. Control of the inheritance of regulatory T cell identity by a cis element in the Foxp3 locus. Cell. 2014; 158:749–763. [PubMed: 25126783]
39. Tran DQ, et al. Analysis of adhesion molecules, target cells, and role of IL-2 in human FOXP3+ regulatory T cell suppressor function. J Immunol. 2009; 182:2929–2938. [PubMed: 19234188]
40. Rudra D, et al. Runx-CBFbeta complexes control expression of the transcription factor Foxp3 in regulatory T cells. Nature immunology. 2009; 10:1170–1177. [PubMed: 19767756]
41. Sojka DK, Bruniquel D, Schwartz RH, Singh NJ. IL-2 secretion by CD4+ T cells in vivo is rapid, transient, and influenced by TCR-specific competition. J Immunol. 2004; 172:6136–6143. [PubMed: 15128800]
42. Shanmugasundaram R, Selvaraj RK. Regulatory T cell properties of chicken CD4+CD25+ cells. J Immunol. 2011; 186:1997–2002. [PubMed: 21242520]
43. Andersen KG, Nissen JK, Betz AG. Comparative Genomics Reveals Key Gain-of-Function Events in Foxp3 during Regulatory T Cell Evolution. Frontiers in immunology. 2012; 3:113. [PubMed: 22590469]

References for methods

44. Rubtsov YP, et al. Regulatory T cell-derived interleukin-10 limits inflammation at environmental interfaces. Immunity. 2008; 28:546–558. [PubMed: 18387831]
45. Anders S, et al. Count-based differential expression analysis of RNA sequencing data using R and Bioconductor. Nature protocols. 2013; 8:1765–1786. [PubMed: 23975260]
46. Bolger AM, Lohse M, Usadel B. Trimmomatic: a flexible trimmer for Illumina sequence data. Bioinformatics. 2014; 30:2114–2120. [PubMed: 24695404]
47. Love MI, Huber W, Anders S. Moderated estimation of fold change and dispersion for RNA-seq data with DESeq2. Genome biology. 2014; 15:550. [PubMed: 25516281]
48. Tarca AL, et al. A novel signaling pathway impact analysis. Bioinformatics. 2009; 25:75–82. [PubMed: 18990722]
49. Maere S, Heymans K, Kuiper M. BiNGO: a Cytoscape plugin to assess overrepresentation of gene ontology categories in biological networks. Bioinformatics. 2005; 21:3448–3449. [PubMed: 15972284]
50. Merico D, Isserlin R, Stueker O, Emili A, Bader GD. Enrichment map: a network-based method for gene-set enrichment visualization and interpretation. PloS one. 2010; 5:e13984. [PubMed: 21085593]

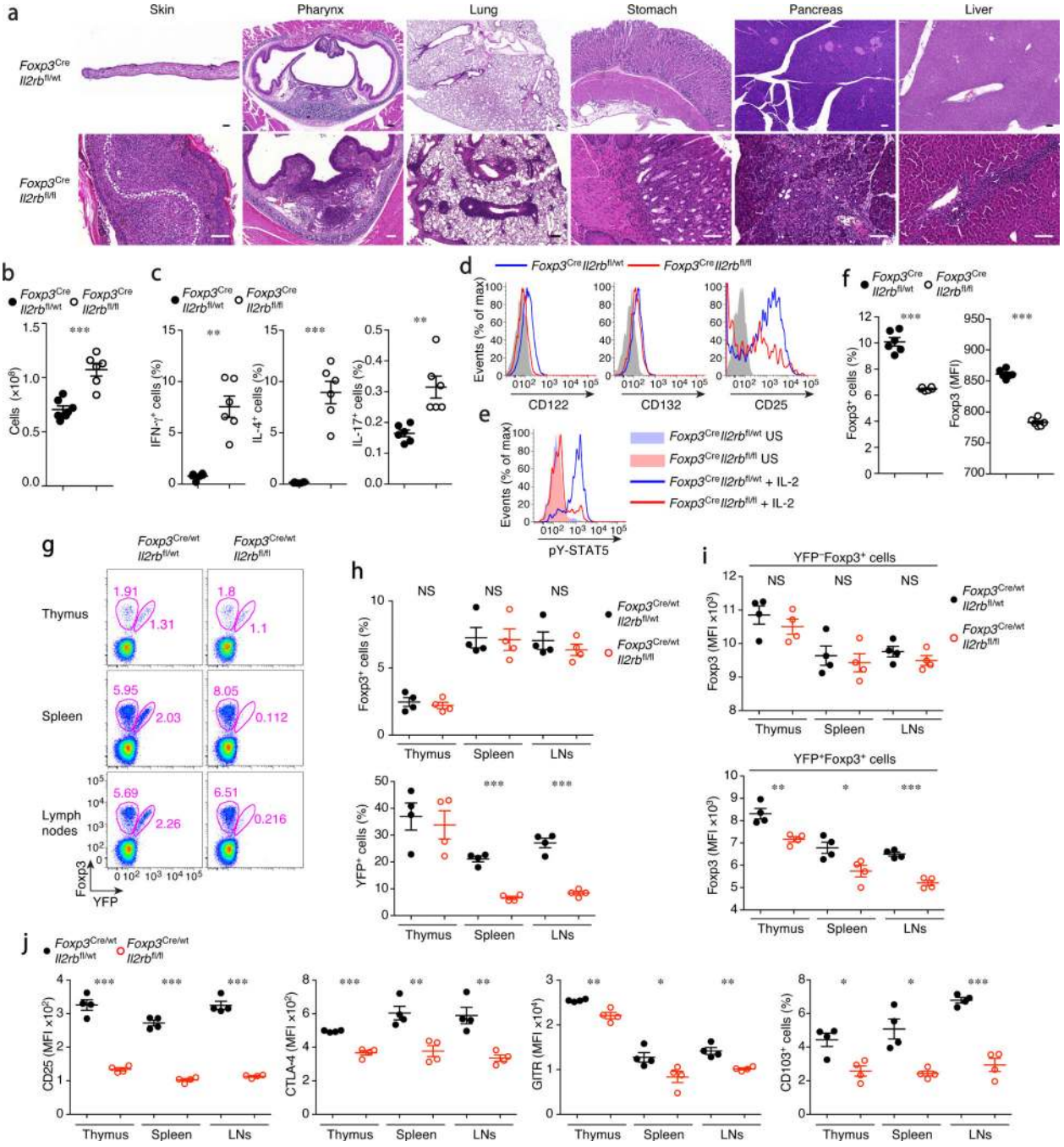

Figure 1.

IL-2Rβ is indispensable for T_{reg} cell function. (**a**) Histopathology of indicated organs of *Foxp3*^{Cre}*Il2rb*$^{fl/wt}$ and *Foxp3*^{Cre}*Il2rb*$^{fl/fl}$ mice. Scale bar, 100 μm. (**b**) Lymph node (LN) cellularity of indicated mice. (**c**) Cytokine production by splenic CD4^{+}Foxp3^{-} cells stimulated for 5 hr with anti-CD3/CD28. (**d**) IL-2R subunit expression by CD4^{+}Foxp3^{+} cells from *Foxp3*^{Cre}*Il2rb*$^{fl/wt}$ (blue) and *Foxp3*^{Cre}*Il2rb*$^{fl/fl}$ (red) mice. (**e**) Intracellular phospho-STAT5 levels in T_{reg} cells from the indicated mice unstimulated (US) or *in vitro* stimulated with rmIL-2 (1,000 U/ml) for 20 min. (**f**) The frequencies of T_{reg} cells among LN

$CD3^+CD4^+$ cells (left) and Foxp3 expression levels (MFI: mean fluorescence intensity) in the $CD3^+CD4^+$ $Foxp3^+$ cells (right). (**g-j**) The analysis of healthy heterozygous female *Foxp3*$^{Cre/wt}$ mice. (**g**) YFP (Cre) expression and intracellular Foxp3 staining identify T_{reg} cells with or without YFP-Cre expression. Gates shown are for $CD3^+CD4^+$ cells. (**h**) The frequencies of $Foxp3^+$ cells among $CD3^+CD4^+$ cells (upper panel) and of Cre expressing cells among $Foxp3^+$ cells (lower panel) in the indicated organs of *Foxp3*$^{Cre/wt}$*Il2rb*$^{fl/wt}$ (black) and *Foxp3*$^{Cre/wt}$*Il2rb*$^{fl/fl}$ (red) mice. (**i**) Foxp3 expression levels (MFI) in YFP^-Foxp3^+ (upper panel) and YFP^+Foxp3^+ (lower panel) cells. (**j**) The expression of indicated markers in YFP^+Foxp3^+ cells. Cells were analyzed by flow cytometry (**b**–**j**). 3–5 wk-old sex and age matched mice were analyzed. *, $P < 0.05$; **, $P < 0.01$; ***, $P < 0.001$; NS, not significant (two-tailed unpaired Student's t test). Data are from one experiment representative of three independent experiments with similar results with three or more mice per group in each (**b**, **c**, **f**, **h**, **i**, **j**; each dot represents a single mouse; mean ± s.e.m.) or representative data of more than five (**a**) or ten (**d**, **e**, **g**) mice per group analyzed are shown.

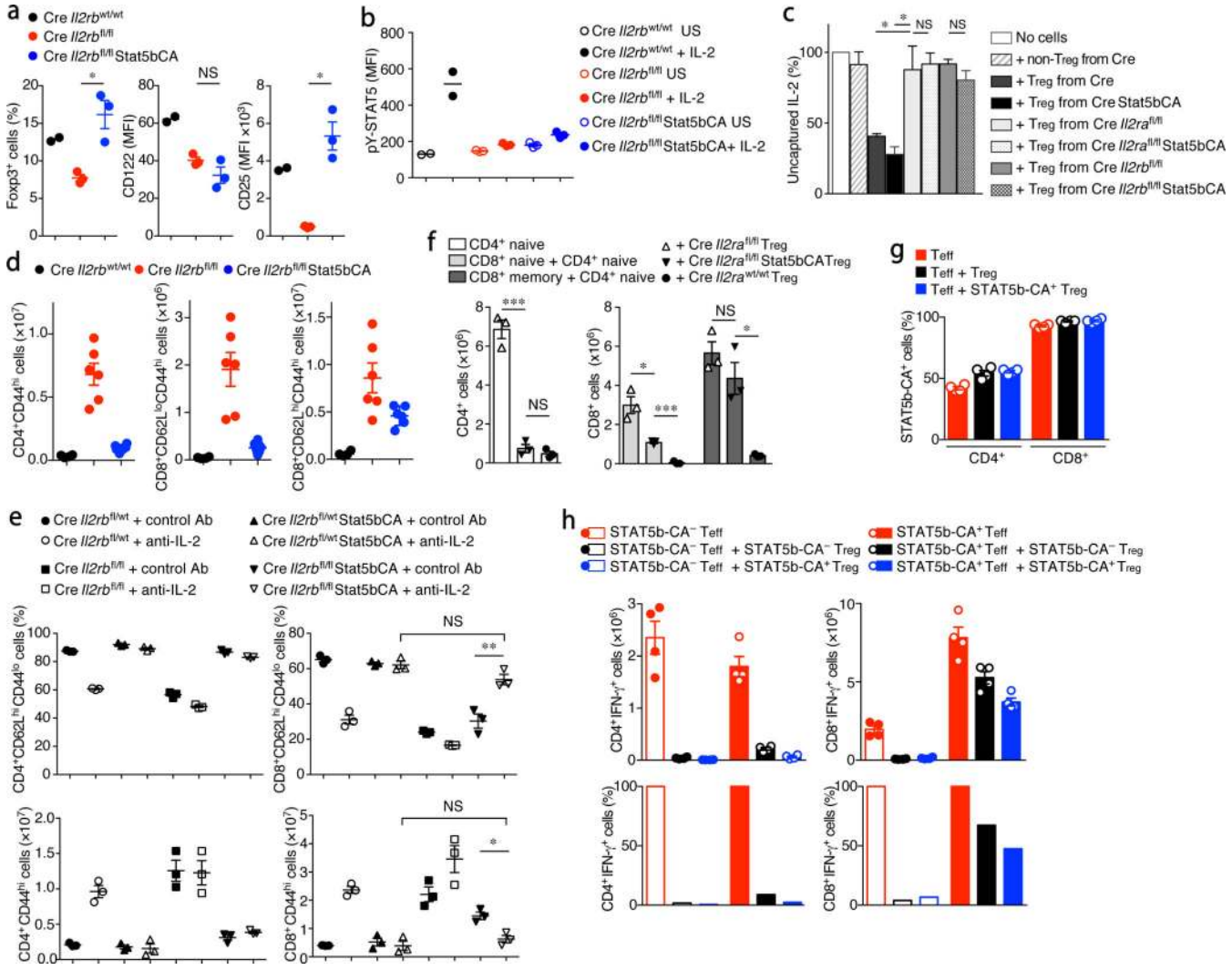

Figure 2.

Restoration of the suppressor activity of IL-2R-deficient T_{reg} cells in the presence of an active form of STAT5. (**a**) The frequencies of Foxp3$^+$ cells among CD3$^+$CD4$^+$ cells and CD122 and CD25 expression by CD3$^+$CD4$^+$Foxp3$^+$ cells. (**b**) Intracellular phospho-STAT5 levels in LN T_{reg} cells from the indicated mice unstimulated (US) or *in vitro* stimulated with rmIL-2 (1,000 U/ml) for 20 min. (**c**) *In vitro* IL-2 capture assay. T_{reg} and non-T_{reg} cells from the indicated mice were sorted and cultured for 2 hr with recombinant human IL-2 (hIL-2). The amount of residual hIL-2 in the media after 2 hr was measured using flow cytometry-based bead array analysis and shown as percent value. (**d**) The cell numbers of indicated CD4$^+$ and CD8$^+$ cell subset (both CD3$^+$Foxp3$^-$) in the LNs of indicated mice (2 wk old). (**e**) The frequencies of naive (CD62L^{hi}CD44^{lo}) T cells among CD3$^+$CD4$^+$Foxp3$^-$ and CD3$^+$CD8$^+$Foxp3$^-$ cells (upper two panels) and the numbers of CD44^{hi} activated CD3$^+$CD4$^+$Foxp3$^-$ and CD3$^+$CD8$^+$Foxp3$^-$ cells (lower two panels) in the LNs of indicated mice treated with IL-2 neutralizing antibodies or control IgG for 2 wks starting from day 5–7 after birth. (**f**) Analysis of the ability of IL-2R-sufficient and -deficient T_{reg} cells to suppress the expansion of naive and activated/memory CD4$^+$ and CD8$^+$ T cells.

$CD4^+Foxp3^-CD62L^{hi}CD44^{lo}$ ($CD4^+$ naive), $CD8^+Foxp3^-CD62L^{hi}CD44^{lo}$ ($CD8^+$ naive), and $CD8^+Foxp3^-CD62L^{hi}CD44^{hi}$ ($CD8^+$ memory) T cells were sorted from *Foxp3*^{Cre} mice and adoptively transferred (1×10^6 cells each) into T cell-deficient (*Tcrb*$^{-/-}$*Tcrd*$^{-/-}$) mice together with T_{reg} cells (2×10^5 cells) sorted from the indicated mice. $CD4^+Foxp3^-$ and $CD8^+Foxp3^-$ T cell numbers in the LNs of recipients 3 wks after transfer are shown. (**g, h**) Analysis of susceptibility of $CD4^+$ and $CD8^+$ T cells expressing an active form of STAT5 to T_{reg} mediated suppression. (**g**) The frequencies of STAT5b-CA-expressing $CD4^+$ and $CD8^+$ T_{eff} cells within total $CD4^+$ and $CD8^+$ T_{eff} cells 3 wks after a transfer of *in vitro* TAT-Cre recombinase treated $CD4^+Foxp3^-$ and $CD8^+Foxp3^-$ T cells sorted from *Foxp3*^{Cre}*Rosa26*^{Stat5bCA} mice and transferred (1×10^6 cells each) into *Tcrb*$^{-/-}$*Tcrd*$^{-/-}$ recipients. (**h**) The numbers and proportion (%) of IFN-γ-producing $CD4^+$ and $CD8^+$ T cells in the recipients without a co-transfer of T_{reg} cells (red bars) or with 2×10^5 control (black bars) or STAT5b-CA-expressing T_{reg} cells (blue bars) sorted from *Foxp3*^{Cre} or *Foxp3*^{Cre}*Rosa26*^{Stat5bCA} mice, respectively. As a control, $CD4^+Foxp3^-$ and $CD8^+Foxp3^-$ T cells sorted from *Foxp3*^{Cre}*Rosa26*^{wt} mice were similarly treated with TAT-Cre and transferred to assess the susceptibility of STAT5b-CA^- T_{eff} cells to T_{reg} mediated suppression (open bars). *, $P < 0.05$; **, $P < 0.01$; ***, $P < 0.001$; NS, not significant (two-tailed unpaired Student's t test). Data are from one experiment representative of two (**b**, **c**, **e**, **f**) or three (**a**, **d**, **g**, **h**) independent experiments with similar results with two or more (**a**, **b**) or three or more (**c**, **d**, **e**, **f**, **g**, **h**) mice per group in each experiment (each dot represents a single mouse; mean ± s.e.m.).

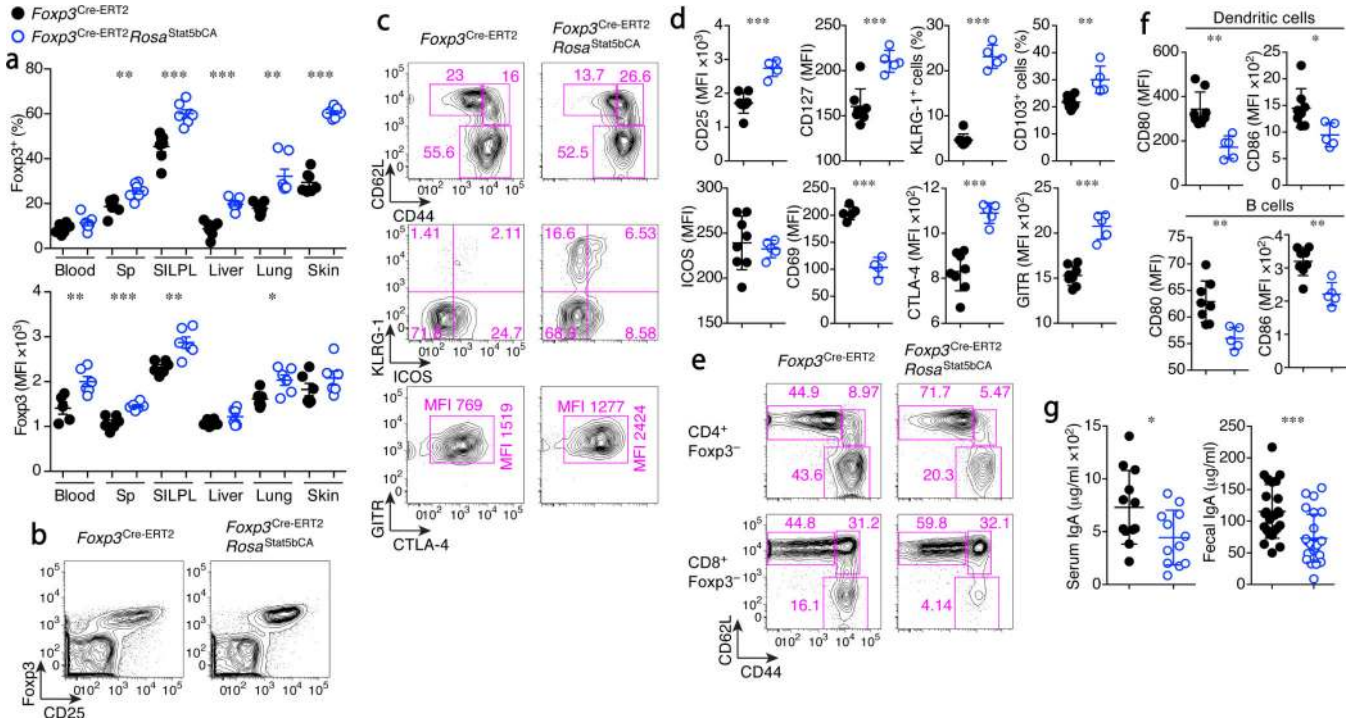

Figure 3.

Increased proliferative and suppressor activity of T_{reg} cells expressing an active form of STAT5. (**a**–**g**) Analysis of *Foxp3*$^{Cre\text{-}ERT2}$ (black dots) and *Foxp3*$^{Cre\text{-}ERT2}$*Rosa26*^{Stat5bCA} (blue dots) mice three months after a single tamoxifen treatment. (**a**) The frequencies of Foxp3$^+$ cells among CD3$^+$CD4$^+$ cells (upper graph) and the expression levels of Foxp3 in CD3$^+$CD4$^+$Foxp3$^+$ cells (lower graph) in the indicated organs. Sp: spleen, SILPL: small intestine lamina propria lymphocytes. (**b**) Analysis of splenic CD4$^+$ T cells for the expression of CD25 and Foxp3. (**c**) Analysis of splenic CD4$^+$Foxp3$^+$ T_{reg} cells. (**d**) The expression of indicated markers in splenic CD4$^+$Foxp3$^+$ T_{reg} cells. (**e**) Analysis of splenic CD3$^+$CD4$^+$Foxp3$^-$ (upper panels) and CD3$^+$CD8$^+$Foxp3$^-$ (lower panels) cells. (**f**) The expression of CD80 and CD86 on DCs (CD11c$^+$MHC class II^{hi}) and B cells (B220$^+$CD11c$^-$) in the LNs. (**g**) Serum and fecal IgA levels as determined by ELISA. Sex and age matched mice were analyzed. Cells were analyzed by flow cytometry (**a**–**f**). *, $P < 0.05$; **, $P < 0.01$; ***, $P < 0.001$ (two-tailed unpaired Student's t test). Data are from one experiment representative of two (**a**, **d**, **f, g**) independent experiments with similar results with five or more mice per group in each experiment (**a**, **d**, **f, g**; each dot represents a single mouse; mean ± s.e.m.) or representative data of more than ten mice per group analyzed are shown (**b**, **c**, **e**).

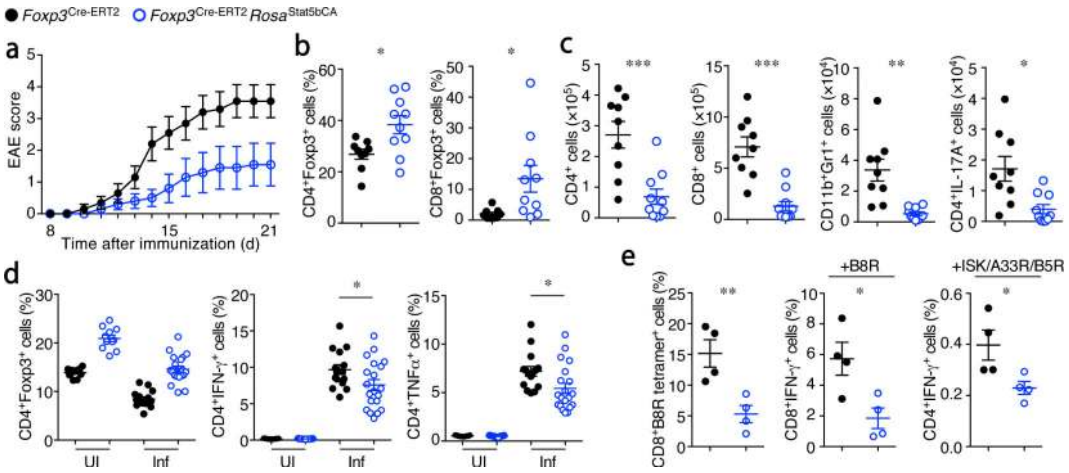

Figure 4.

Potent suppressor function of T_{reg} cells expressing an active form of STAT5. (**a**–**c**) Analysis of EAE induced upon immunization with MOG peptide in CFA. (**a**) Average disease scores (n=10 each). (**b**) The frequencies $Foxp3^+$ cells among brain-infiltrating $CD3^+CD4^+$ (left) and $CD3^+CD8^+$ (right) cells in mice shown in (**a**). (**c**) The numbers of the indicated brain-infiltrating cells in mice shown in (**a**). (**d**) T cell responses against *Listeria monocytogenes* in uninfected (UI) or infected (Inf; day 8 after infection) mice. The frequencies of $Foxp3^+$ T_{reg} cells among $CD3^+CD4^+$ cells (left). The frequencies of IFN-γ (middle) and TNFα (right) producing $CD4^+TCR\beta^+Foxp3^-$ cells after 5 hr *in vitro* re-stimulation with heat-killed *Listeria* in the presence of DCs. (**e**) Anti-viral T cell responses in mice on day 8 after infection with non-replicating vaccinia virus. The frequencies of vaccinia B8R peptide-specific $CD8^+$ T cells detected using H-$2K^b$-B8R tetramer (left), IFN-γ production by $CD8^+Foxp3^-$ (middle) and $CD4^+Foxp3^-$ (right) cells after a 5 hr *in vitro* stimulation with B8R peptide or a mixture of three vaccinia virus-specific peptides (ISK, A33R, and B5R). Cells were analyzed by flow cytometry (**b**–**e**). Sex and age matched *Foxp3*$^{Cre\text{-}ERT2}$ (black) and *Foxp3*$^{Cre\text{-}ERT2}$*Rosa26*^{Stat5bCA} (blue) mice were challenged or infected as indicated 2-3 months after a single tamoxifen treatment. *, $P < 0.05$; **, $P < 0.01$; ***, $P < 0.001$ (two-tailed unpaired Student's t test). Data are from one experiment representative of two independent experiments with similar results with ten (**a**–**c**) or four (**e**) mice per group in each experiment, or pooled from four independent experiments with n=11 (UI), n=15 (Inf, control), or n=20 (Inf, *Rosa26*^{Stat5bCA}) mice per group are shown (**d**). Each dot represents a single mouse (**b**–**e**). mean ± s.e.m. (**a**–**e**).

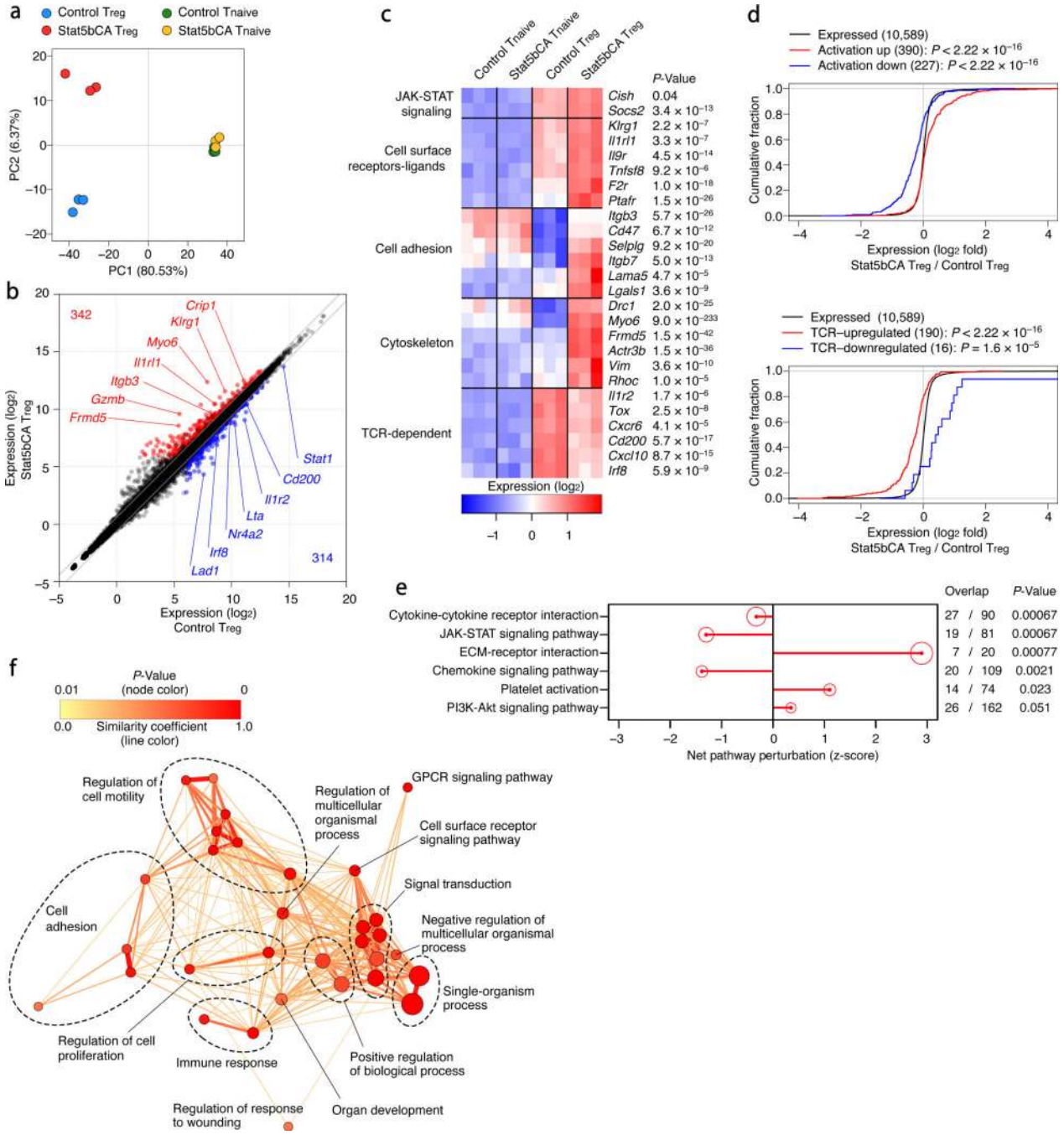

Figure 5.

RNA-seq analysis of T_{reg} cells expressing an active form of STAT5. (**a**) Principal component analysis of RNA-seq datasets, using the top 15% of genes with the highest variance. Each dot represents an RNA sample from a single mouse. Note that "Stat5bCA T naive" cells are T naive cells sorted from tamoxifen-treated *Foxp3*$^{\text{Cre-ERT2}}$*Rosa26*$^{\text{Stat5bCA}}$ mice and do not express STAT5b-CA. Only "Stat5bCA T_{reg}" cells express STAT5b-CA in the four groups of cells presented. (**b**) Plot of gene expression (as $\log_2$ normalized read count) in control vs. STAT5b-CA expressing T_{reg} cells. The diagonal lines indicate fold change of at least 1.5× or

0.67× fold. Significantly up- and down-regulated genes (defined as genes with at least 1.5× or 0.67× fold change, adjusted *P*-value ≤0.05, and expression above a minimal threshold based on the distribution of all genes) are colored red or blue, respectively, and their numbers are shown. (**c**) Heat map of selected genes. Three replicates are shown in order. *P*-values are for control T_{reg} vs. STAT5b-CA expressing T_{reg} cells. (**d**) The empirical cumulative distribution function (ECDF) for the $\log_2$ fold change of all expressed genes in STAT5b-CA vs. control T_{reg} cells, is plotted along with ECDFs for the subsets of genes up- or down-regulated by inflammatory activation in T_{reg} cells[33] (upper graph), or the subsets of genes up- or down-regulated in a TCR-dependent manner in $CD44^{hi}$ T_{reg} cells[34] (lower graph). (**e**) Signaling Pathway Impact Analysis (SPIA) of KEGG pathways. The 6 most statistically significant pathways that show enrichment among differentially expressed (DE) genes in STAT5b-CA vs. control T_{reg} cells are shown. The net pathway perturbation indicates the status of the pathway (positive = activated; negative = inhibited) based on the activating or inhibitory relationships of DE genes within the pathway. The size of the red circle is proportional to the degree of enrichment, and the FDR-adjusted global *P*-value reflecting both enrichment and perturbation is shown. (**f**) Network analysis of GO term enrichment among significantly upregulated genes in STAT5b-CA vs. control T_{reg} cells. Upregulated genes were analyzed for over-represented GO terms using BiNGO in Cytoscape, and the resulting network was calculated and visualized using EnrichmentMap. Groups of similar GO terms (**Supplementary Table 1**) were manually circled. Line thickness and color are proportional to the similarity coefficient between connected nodes. Node color is proportional to the FDR-adjusted *P*-value of the enrichment. Node size is proportional to gene set size.

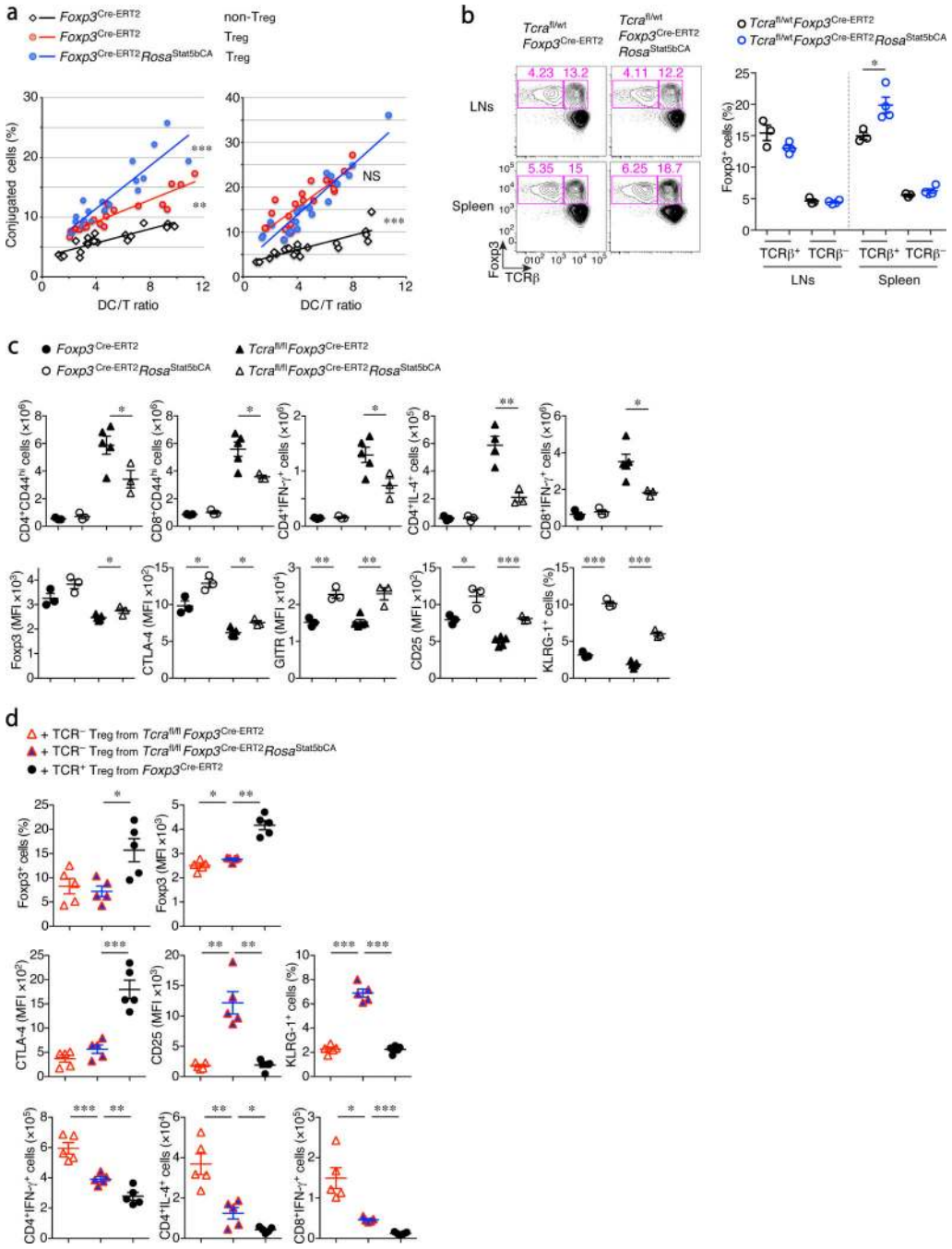

Figure 6.

Augmented STAT5 signaling in T_{reg} cells increases the conjugate formation between T_{reg} cells and DCs and potentiates suppressor function in a TCR independent manner. (**a**) Analysis of *in vitro* conjugate formation between T cells and DCs. CFSE-labeled T_{reg} and non-T_{reg} cells from the indicated mice were co-cultured with graded numbers of CellTrace Violet-labeled $CD11c^+$ DCs from C57BL/6J mice for 720 min in the absence (left panel) or presence (right panel) of rmIL-2 (100 IU/ml). Each dot represents a flow cytometric analysis of conjugate formation in a single well. (**b**) Expression of Foxp3 and TCRβ by $CD4^+$ cells in

the LNs and spleen of *Tcra*$^{fl/wt}$ heterozygous mice treated with tamoxifen for 2 wks. The frequencies of TCR-sufficient and -deficient Foxp3$^+$ cells among CD4$^+$ cells are summarized in the right panel. (**c**) T cell activation and pro-inflammatory cytokine production in the LNs of indicated mice treated with tamoxifen for 2 wks. The lower five panels show the expression of the indicated molecules in LN T_{reg} cells. (**d**) The analysis of T cells transferred into *Tcrb*$^{-/-}$ *Tcrd*$^{-/-}$ recipients. WT CD4$^+$Foxp3$^-$ and CD8$^+$Foxp3$^-$ T cells (5×10^5 cells each) were transferred together with TCR-ablated (TCRβ^{lo}CD3^{lo}) or TCR-sufficient T_{reg} cells (3×10^5 cells) sorted from the indicated mice that had been treated with tamoxifen for 2 wks. The frequencies of T_{reg} cells and Foxp3 expression levels in T_{reg} cells (upper two panels), the expression of the indicated molecules in T_{reg} cells (middle three), and the numbers of cytokine producing CD4$^+$ and CD8$^+$ T cells (lower three) in the LNs of recipient mice 3 wks after the transfer are shown. Sex and age matched mice were analyzed. Cells were analyzed by flow cytometry (**a**–**d**). *, $P < 0.05$; **, $P < 0.01$; ***, $P < 0.001$ (modified ANCOVA in Prism software (**a**) or two-tailed unpaired Student's t test (**b**, **c**, **d**)). Data are from one experiment representative of three (**a**) or two (**b**, **d**) or four (**c**) independent experiments with similar results with three or more (**b**, **c**) or five or more (**d**) mice per group in each experiment (**b**, **c**, **d**; each dot represents a single mouse; mean ± s.e.m.).